MethodsX 9 (2022) 101905

Contents lists available at ScienceDirect

MethodsX

journal homepage: www.elsevier.com/locate/mex

Method Article

High order approximation on non-uniform meshes for generalized time-fractional telegraph equation

Farheen Sultana [a], Rajesh K. Pandey [a,*], Deeksha Singh [a], Om P. Agrawal [b]

[a] Department of Mathematical Sciences, Indian Institute of Technology (BHU) Varanasi, Varanasi, 221005, Uttar Pradesh, India

[b] Mechanical Engineering and Energy Processes, Southern Illinois University, Carbondale, IL-62901, USA

A B S T R A C T

This paper presents a high order approximation scheme to solve the generalized fractional telegraph equation (GFTE) involving the generalized fractional derivative (GFD). The GFD is characterized by a scale function $\sigma(t)$ and a weight function $\omega(t)$. Thus, we study the solution behavior of the GFTE for different $\sigma(t)$ and $\omega(t)$. The scale function either stretches or contracts the solution while the weight function dramatically shifts the numerical solution of the GFTE. The time fractional GFTE is approximated using quadratic scheme in the temporal direction and the compact finite difference scheme in the spatial direction. To improve the numerical scheme's accuracy, we use the non-uniform mesh. The convergence order of the whole discretized scheme is, $O(\tau^{2\alpha-3}, h^4)$, where τ and h are the temporal and spatial step sizes respectively. The outcomes of the work are as follows:

- The error estimate for approximation of the GFD on non-uniform meshes is established.
- The numerical scheme's stability and convergence are examined.
- Numerical results for four examples are compared with those obtained using other method. The study shows that the developed scheme achieves higher accuracy than the scheme discussed in literature.

A R T I C L E I N F O

Method name: High order approximation on non-uniform meshes for generalized time-fractional telegraph equation
Keywords: Generalized fractional derivative, Generalized fractional telegraph equations, High order scheme, Non-uniform mesh, Stability and convergence
Article history: Available online 4 November 2022

* Corresponding author.
E-mail addresses: farheen.sultana.rs.mat18@itbhu.ac.in (F. Sultana), rkpandey.mat@iitbhu.ac.in (R.K. Pandey), deeksha.singh.rs.mat18@itbhu.ac.in (D. Singh), om@engr.siu.edu, bz.man2@gmail.com (O.P. Agrawal).

https://doi.org/10.1016/j.mex.2022.101905

Specifications table

Subject Area:	Mathematics
More specific subject area:	Numerical solution of fractional partial differential equations
Method name:	High order approximation on non-uniform meshes for generalized time-fractional telegraph equation
Name and reference of original method:	NA
Resource availability:	NA

Introduction

Fractional calculus has gained much interest in the past few decades. Fractional calculus has many applications in diverse areas of science and engineering, such as biology [1], physics [2], signal processing [3], and viscoelasticity [4]. Readers may see references [5–7] for more information on fractional calculus theory and its applications. In recent years, many researchers studied the various numerical schemes for solving fractional integro-differential equations [8,9], and fractional partial differential equations [10–14]. In this paper, we study a quadratic scheme to approximate GFD and fourth order compact difference scheme to approximate GFTE. The numerical scheme is based on non-uniform meshes. A telegraph equation (TE) is a hyperbolic partial differential equation that arises in many fields, including neutron transport [15], anomalous diffusion [16], wave propagation [17], signal analysis [18], etc. When a TE contains a fractional time derivative term, it is called a fractional telegraph equation. In recent years, many researchers have studied fractional TEs. In [19], the authors examined a finite difference method to deal with fractional TE. Momani [20] proposed an Adomian decomposition method to solve the space and time-fractional TE. In [21], the author presented a fundamental solution of time-fractional TE. Dehghan and Shokri [22] applied a collocation point method to solve hyperbolic TE. Chen et al. [23] solved the Riesz space-fractional TE using an unconditional stable difference scheme. Several fractional derivatives have been presented, namely Riemann-Liouville, Caputo, Reisz, Riesz-Riemann, Riesz-Caputo, etc. Agrawal [24] used a generalized fractional derivative to develop formulations for fractional variational calculus. This GFD incorporates a scale function $\sigma(t)$ and a weight function $\omega(t)$, which have practical applications. Firstly, $\sigma(t)$ allows the time domain to be expanded or contracted. In typical cases, this reduces the computational time and captures the phenomena over a few seconds. Secondly, $\omega(t)$ makes it possible to measure the incident differently at various time points. In this paper, we develop a numerical scheme for the GFTEs. A GFTE is of more importance than fractional TE due to the involvement of $\omega(t)$ and $\sigma(t)$. There are only a few papers on the numerical approximation of generalized fractional differential equations. Xu et al. [25–28] have studied finite difference method to approximate GFDs. Yadav et al. [29] presented a Taylor approximation for the discretization of GFDs. Kumar et al. [30] discussed a numerical solution of the generalized fractional telegraph equations. Due to the presence of the non-singular term in the definition of fractional integrals and derivatives, the accuracy of L1 approximation (10) (defined later) depends on fractional-order α [30]. Also, for $s \to t$, $(\sigma(t) - \sigma(s))^{m-\alpha-1} \to 0$. So, for a better approximation, we take small step sizes close to the singular point, while large step sizes away from the singular point. Hence, to improve the accuracy of fractional derivatives, non-uniform meshes are added. In [31–34], the authors solved the fractional diffusion and diffusion wave equations using discretization schemes on non-uniform meshes. Previously, the research of GFDs was restricted to uniform meshes in both the temporal and spatial directions. To the best of our knowledge, the GFTE on non-uniform mesh has never been investigated. So, we attempt to fill this gap and apply high order scheme to approximate the GFTE on non-uniform meshes. The following is an outline of the paper: Firstly in Section “Preliminaries”, we present some definitions of fractional integrals, derivatives, and generalized derivatives of fractional order. In Section “Problem formulation”, we approximate the GFDs using quadratic interpolation approximation on non-uniform meshes and derive an error estimate of GFDs. We apply a high order compact difference scheme to approximate GFTE on non-uniform meshes and present matrix form for the scheme in Section “A fourth-order compact difference scheme”. We discuss the stability and convergence of the scheme in

Section “Stability and convergence analysis”. In Section “Numerical results”, we present four numerical examples to support the theoretical findings.

Preliminaries

Here, we give some basic definitions of fractional derivatives and integrals. Additional detail of fractional derivatives can be found in [5–7].

Definition 1. Let $\alpha \in \mathbb{R}^+$, the classical Riemann-Liouville integral of fractional order α of a function $v(t)$ is as follows

$$I^{\alpha} v(t) = \frac{1}{\Gamma(\alpha)} \int_0^t (t-s)^{\alpha-1} v(s) ds, \quad t > 0. \tag{1}$$

Definition 2. The classical Caputo derivative of fractional order α of a function $v(t)$ is as follows

$$D^{\alpha} v(t) = D^k I^{k-\alpha} v(t) = \frac{1}{\Gamma(k-\alpha)} \int_0^t (t-s)^{k-\alpha-1} v^{(k)}(s) ds, \quad t > 0, \tag{2}$$

where $k-1 \le \alpha < k$, $k \in \mathbb{N}^+$.

Following Eqs. (1)-(2), we give some definitions of GFDs. Here, the classical first order derivative with respect to t is denoted by D_t and prime indicates the derivative.

Definition 3. [24] Let $\alpha \in \mathbb{R}^+$, the left generalized integral of order α of a function $v(t)$ is defined as

$$I^{\alpha}_{0+;[\sigma;\omega]} v(t) = \frac{[\omega(t)]^{-1}}{\Gamma(\alpha)} \int_0^t \frac{\omega(s)\sigma'(s)v(s)}{[\sigma(t)-\sigma(s)]^{1-\alpha}} ds, \tag{3}$$

provided the integral exists.

Definition 4. [24] Let $k \in \mathbb{N}^+$, the left generalized derivative of kth order of a function $v(t)$ is defined as

$$D^{k}_{[L;\sigma;\omega]} v(t) = \frac{1}{\omega(t)} \left[\left(\frac{1}{\sigma'(t)} D_t \right)^k (v(t)\omega(t)) \right], \tag{4}$$

Definition 5. [24] Let $\alpha \in \mathbb{R}^+$, the left generalized derivative of α order of function $v(t)$ is defined as

$$D^{\alpha}_{0+;[\sigma;\omega;2]} v(t) = I^{k-\alpha}_{0+;[\sigma;\omega]} D^{k}_{[L;\sigma;\omega]} v(t), \tag{5}$$

assuming the right-side of the Eq. (5) is finite, where $k-1 \le \alpha < k$, and $k \in \mathbb{N}^+$.

For $k = 1$, i.e. $\alpha \in (0,1)$, the GFD in Eq. (5) will be given as,

$${}^{*}\mathbb{D}^{\alpha} v(t) = D^{\alpha}_{0+;[\sigma;\omega;2]} v(t) = \frac{[\omega(t)]^{-1}}{\Gamma(1-\alpha)} \int_0^t \frac{[v(s)\omega(s)]'}{(\sigma(t)-\sigma(s))^{\alpha}} ds. \tag{6}$$

In the above definitions, we only define the left generalized fractional integral and GFDs. The right generalized fractional integral and GFDs can be studied from [24].

Problem formulation

Consider the following GFTE given by,

$$\frac{{}^{*}\partial^{2\alpha} v(x,t)}{{}^{*}\partial t^{2\alpha}} + 2\beta \frac{{}^{*}\partial^{\alpha} v(x,t)}{{}^{*}\partial t^{\alpha}} = \kappa^2 \frac{\partial^2 v(x,t)}{\partial x^2} + f(x,t), \tag{7}$$

where $\kappa, \beta > 0$, $\alpha \in (0, 1/2]$, and $f(x,t)$ is a force term. Here $\frac{{}^{*}\partial^{2\alpha} v(x,t)}{{}^{*}\partial t^{2\alpha}}$ and $\frac{{}^{*}\partial^{\alpha} v(x,t)}{{}^{*}\partial t^{\alpha}}$ denotes the GFD.

Here, we discuss a fourth-order compact difference scheme for solving the GFTE (7) using the following initial and boundary conditions,

$$v(x,0) = \phi(x), \quad x \in [a,b], \tag{8}$$

$$v(a,t) = g_1(t), \quad v(b,t) = g_2(t), \quad 0 < t \le T. \tag{9}$$

Equation (7) together with Eqs. (8) and (9) provide a model to solve GFTE.

The standard scheme for approximating the GFD is as follows [30]:

$$[{}^*\mathbb{D}^{\alpha} v(t)]_{t_n} = \frac{[\omega(t_n)]^{-1}}{\Gamma(1-\alpha)} \sum_{k=1}^{n} \frac{\omega(t_k)v(x,t_k) - \omega(t_{k-1})v(x,t_{k-1})}{t_k - t_{k-1}} \int_{t_{k-1}}^{t_k} [\sigma(t_n) - \sigma(s)]^{-\alpha} ds + R^n, \tag{10}$$

where $0 = t_0 < t_1 < \cdots < t_n$, and R^n is the local error of truncation. It has been demonstrated that $R^n = O(\tau^{2-\alpha})$ [30] in the situation of uniform mesh, i.e., $t_k - t_{k-1} = \tau$, $k = 1, 2, \ldots, n$.

For non-uniform mesh, we divide the interval $[0, T]$ into subintervals with $0 = t_0 < t_1 < \cdots < t_N = T$, where N is an integer. Let the time step be denoted as $\tau_n = t_n - t_{n-1}$, $1 \le n \le N$. The non-uniform mesh [32] is defined as

$$\tau_n = (N + 1 - n)\mu, \quad 1 \le n \le N \tag{11}$$

where $\mu = \frac{2T}{N(N+1)}$. The non-uniform mesh has a larger grid spacing near $t_0 = 0$, and small grid spacing near $t_N = T$. We aim to solve Eq. (7) on non-uniform mesh defined by Eq. (11).

Approximation of GFDs on non-uniform meshes

We derive a quadratic interpolation approximation to approximate the GFDs on non-uniform mesh. Define the non-uniform meshes on interval $[0, T]$ with $0 = t_0 < t_1 < \cdots < t_N = T$, where N is an integer and $t_n, 1 \le n \le N$ is defined using the scheme discussed in the above section. For simplicity, we use the notations $\omega(t_k) = \omega_k$, $\sigma(t_k) = \sigma_k$, and $v(t_k) = v_k$.

For each small interval $[t_{k-1}, t_k](1 \le k \le n)$, the linear interpolation approximation of function $v(t)\omega(t)$ by using node points $(t_{k-1}, v_{k-1}\omega_{k-1})$ and $(t_k, v_k\omega_k)$ is denoted as $p_k^1(t)$, i.e.

$$p_k^1(t) = \sum_{l=k-1}^{k} \Big(\prod_{j=k-1, j\neq l}^{k} \frac{(t - t_j)}{(t_l - t_j)} \Big) v_l\omega_l,$$
$$(p_k^1(t))' = \frac{v_k\omega_k - v_{k-1}\omega_{k-1}}{\tau_k}. \tag{12}$$

For $k \ge 2$, on each small interval $[t_{k-1}, t_k]$, the quadratic interpolation approximation of function $v(t)\omega(t)$, by using node points $(t_{k-2}, v_{k-2}\omega_{k-2})$, $(t_{k-1}, v_{k-1}\omega_{k-1})$, $(t_k, v_k\omega_k)$ is denoted as $p_k^2(t)$, i.e.

$$p_k^2(t) = \sum_{l=k-2}^{k} \Big(\prod_{j=k-2, j\neq l}^{k} \frac{(t - t_j)}{(t_l - t_j)} \Big) v_l\omega_l,$$
$$= p_k^1(t) + \frac{(t - t_k)(t - t_{k-1})}{t_k - t_{k-2}} \left[\frac{v_k\omega_k - v_{k-1}\omega_{k-1}}{t_k - t_{k-1}} - \frac{v_{k-1}\omega_{k-1} - v_{k-2}\omega_{k-2}}{t_{k-1} - t_{k-2}} \right],$$
$$(p_k^2(t))' = \frac{v_k\omega_k - v_{k-1}\omega_{k-1}}{\tau_k} + (2t - (t_k + t_{k-1}))\mathcal{D}_t v_k\omega_k, \tag{13}$$

where,

$$\mathcal{D}_t v_k\omega_k = \frac{1}{t_k - t_{k-2}} \left[\frac{v_k\omega_k - v_{k-1}\omega_{k-1}}{t_k - t_{k-1}} - \frac{v_{k-1}\omega_{k-1} - v_{k-2}\omega_{k-2}}{t_{k-1} - t_{k-2}} \right].$$

Therefore, the first generalized fractional derivative term of Eq. (7) can be discretized as:

$$\frac{{}^*\partial^{2\alpha} v(x_i, t_n)}{{}^*\partial t^{2\alpha}} = \frac{[\omega(t_n)]^{-1}}{\Gamma(1 - -2\alpha)} \sum_{k=1}^{n} \int_{t_{k-1}}^{t_k} \frac{1}{[\sigma(t_n) - \sigma(s)]^{2\alpha}} (v(s)\omega(s))' ds, \tag{14}$$

$$= \frac{[\omega(t_n)]^{-1}}{\Gamma(1-2\alpha)}\Big[\int_{t_0}^{t_1}\frac{1}{[\sigma(t_n)-\sigma(s)]^{2\alpha}}(p_k^1(s))'ds + \sum_{k=2}^{n}\int_{t_{k-1}}^{t_k}\frac{1}{[\sigma(t_n)-\sigma(s)]^{2\alpha}}(p_k^2(s))'ds\Big], \tag{15}$$

$$\begin{aligned}
&= \frac{[\omega(t_n)]^{-1}}{\Gamma(1-2\alpha)}\Big[\frac{v_1\omega_1 - v_0\omega_0}{\tau_1}\int_{t_0}^{t_1}[\sigma(t_n)-\sigma(s)]^{-2\alpha}ds + \sum_{k=2}^{n}\int_{t_{k-1}}^{t_k}\\
&\quad\times[\sigma(t_n)-\sigma(s)]^{-2\alpha}\Big[\frac{v_k\omega_k - v_{k-1}\omega_{k-1}}{\tau_k} + (2s-(t_k+t_{k-1}))\mathcal{D}_t v_k\omega_k\Big]ds\Big],\\
&= \frac{[\omega(t_n)]^{-1}}{\Gamma(1--2\alpha)}\Big[\sum_{k=1}^{n}\frac{v_k\omega_k - v_{k-1}\omega_{k-1}}{\tau_k}\int_{t_{k-1}}^{t_k}[\sigma(t_n)-\sigma(s)]^{-2\alpha}ds\\
&\quad+\sum_{k=2}^{n}\mathcal{D}_t v_k\omega_k\int_{t_{k-1}}^{t_k}[\sigma(t_n)-\sigma(s)]^{-2\alpha}(2s-(t_k+t_{k-1}))ds\Big],\\
&= \sum_{k=1}^{n}A_k^n(v_k\omega_k - v_{k-1}\omega_{k-1}) + \frac{1}{\Gamma(2-2\alpha)}\sum_{k=2}^{n}B_k^n\mathcal{D}_t v_k\omega_k,\\
&= \sum_{k=1}^{n}A_k^n(v_k\omega_k - v_{k-1}\omega_{k-1}) + \frac{1}{\Gamma(2-2\alpha)}\Big[\sum_{k=2}^{n}B_k^n\frac{1}{\tau_{k-1}+\tau_k}\frac{1}{\tau_k}\\
&\quad\times(v_k\omega_k - v_{k-1}\omega_{k-1}) - \sum_{k=1}^{n-1}B_{k+1}^n\frac{1}{\tau_k+\tau_{k+1}}\frac{1}{\tau_k}(v_k\omega_k - v_{k-1}\omega_{k-1})\Big],\\
&= \sum_{k=1}^{n}C_k^n(v_k\omega_k - v_{k-1}\omega_{k-1}),
\end{aligned} \tag{16}$$

where, $C_1^1 = A_1^1$, for $n = 1$. For $n \geq 2$,

$$C_k^n = \begin{cases} A_1^n - \frac{1}{\Gamma(2-2\alpha)}\frac{1}{\tau_1+\tau_2}\frac{1}{\tau_1}B_2^n, & k = 1,\\ A_k^n + \frac{1}{\Gamma(2-2\alpha)}\Big(\frac{1}{\tau_{k-1}+\tau_k}\frac{1}{\tau_k}B_k^n - \frac{1}{\tau_k+\tau_{k+1}}\frac{1}{\tau_k}B_{k+1}^n\Big), & 2 \leq k \leq n-1,\\ A_n^n + \frac{1}{\Gamma(2-2\alpha)}\frac{1}{\tau_{n-1}+\tau_n}\frac{1}{\tau_n}B_n^n, & k = n. \end{cases} \tag{17}$$

Also,

$$A_k^n = \frac{[\omega(t_n)]^{-1}}{\Gamma(1-2\alpha)}\frac{1}{\tau_k}\int_{t_{k-1}}^{t_k}[\sigma(t_n)-\sigma(s)]^{-2\alpha}ds,$$

$$B_k^n = (1-2\alpha)[\omega(t_n)]^{-1}\int_{t_{k-1}}^{t_k}[\sigma(t_n)-\sigma(s)]^{-2\alpha}(2s-(t_k+t_{k-1}))ds.$$

Now, for solving A_k^n and B_k^n, let

$$\begin{aligned}
&H = [\sigma(t_n)-\sigma(s)],\\
&\Rightarrow dH = -\sigma'(s)ds,\\
&\Rightarrow dH = -\Big(\frac{\sigma(t_k)-\sigma(t_{k-1})}{t_k-t_{k-1}}\Big)ds, \qquad s \in (t_k, t_{k-1}),
\end{aligned}$$

then,

$$A_k^n = \frac{[\omega(t_n)]^{-1}}{\Gamma(2-2\alpha)}\frac{[\sigma(t_n)-\sigma(t_{k-1})]^{1-2\alpha} - [\sigma(t_n)-\sigma(t_k)]^{1-2\alpha}}{[\sigma(t_k)-\sigma(t_{k-1})]}, \quad 1 \leq k \leq n, \tag{18}$$

and

$$B_k^n = [\omega(t_n)]^{-1}\tau_k^2\Big[\frac{2}{(2-2\alpha)}\frac{[\sigma(t_n)-\sigma(t_{k-1})]^{2-2\alpha}-[\sigma(t_n)-\sigma(t_k)]^{2-2\alpha}}{[\sigma(t_k)-\sigma(t_{k-1})]^2} - \frac{[\sigma(t_n)-\sigma(t_{k-1})]^{1-2\alpha}+[\sigma(t_n)-\sigma(t_k)]^{1-2\alpha}}{[\sigma(t_k)-\sigma(t_{k-1})]}\Big], \qquad 2 \le k \le n. \tag{19}$$

Similarly, the second generalized fractional derivative term of Eq. (7) can be discretized as:

$$\frac{{}^*\partial^\alpha v(x_i,t_n)}{{}^*\partial t^\alpha} = \sum_{k=1}^{n} R_k^n(v_k\omega_k - v_{k-1}\omega_{k-1}), \tag{20}$$

where, $R_1^1 = P_1^1$, for $n = 1$. For $n \ge 2$,

$$R_k^n = \begin{cases} P_1^n - \frac{1}{\Gamma(2-\alpha)}\frac{1}{\tau_1+\tau_2}\frac{1}{\tau_1}Q_2^n, & k = 1, \\ P_k^n + \frac{1}{\Gamma(2-\alpha)}\Big(\frac{1}{\tau_{k-1}+\tau_k}\frac{1}{\tau_k}Q_k^n - \frac{1}{\tau_k+\tau_{k+1}}\frac{1}{\tau_k}Q_{k+1}^n\Big), & 2 \le k \le n-1, \\ P_n^n + \frac{1}{\Gamma(2-\alpha)}\frac{1}{\tau_{n-1}+\tau_n}\frac{1}{\tau_n}Q_n^n, & k = n. \end{cases} \tag{21}$$

Also,

$$P_k^n = \frac{[\omega(t_n)]^{-1}}{\Gamma(1-\alpha)}\frac{1}{\tau_k}\int_{t_{k-1}}^{t_k}[\sigma(t_n)-\sigma(s)]^{-\alpha}ds,$$

$$Q_k^n = (1-\alpha)[\omega(t_n)]^{-1}\int_{t_{k-1}}^{t_k}[\sigma(t_n)-\sigma(s)]^{-\alpha}(2t-(t_k+t_{k-1}))ds,$$

then, we have

$$P_k^n = \frac{[\omega(t_n)]^{-1}}{\Gamma(2-\alpha)}\frac{[\sigma(t_n)-\sigma(t_{k-1})]^{1-\alpha}-[\sigma(t_n)-\sigma(t_k)]^{1-\alpha}}{[\sigma(t_k)-\sigma(t_{k-1})]}, \quad 1 \le k \le n, \tag{22}$$

and,

$$Q_k^n = [\omega(t_n)]^{-1}\tau_k^2\Big[\frac{2}{(2-\alpha)}\frac{[\sigma(t_n)-\sigma(t_{k-1})]^{2-\alpha}-[\sigma(t_n)-\sigma(t_k)]^{2-\alpha}}{[\sigma(t_k)-\sigma(t_{k-1})]^2} - \frac{[\sigma(t_n)-\sigma(t_{k-1})]^{1-\alpha}+[\sigma(t_n)-\sigma(t_k)]^{1-\alpha}}{[\sigma(t_k)-\sigma(t_{k-1})]}\Big], \qquad 2 \le k \le n. \tag{23}$$

Now, from discretization of first and second generalized time fractional derivative terms, we have

$$\begin{aligned} &\frac{{}^*\partial^{2\alpha}v(x_i,t_n)}{{}^*\partial t^{2\alpha}} + 2\beta\frac{{}^*\partial^\alpha v(x_i,t_n)}{{}^*\partial t^\alpha} \\ &= \sum_{k=1}^{n} C_k^n(v_k\omega_k - v_{k-1}\omega_{k-1}) + 2\beta\sum_{k=1}^{n} R_k^n(v_k\omega_k - v_{k-1}\omega_{k-1}), \\ &= \sum_{k=1}^{n} a_k^n(v_k\omega_k - v_{k-1}\omega_{k-1}), \end{aligned} \tag{24}$$

where, $a_k^n = C_k^n + 2\beta R_k^n$.

Lemma 1. *Let $\alpha \in [0, \frac{1}{2}]$, the weight function $\omega(t) > 0$ increases monotonically, and the scale function $\sigma(t) > 0$ increases strictly monotonically, then $A_k^n > 0$, $B_k^n > 0$, $P_k^n > 0$ and $Q_k^n > 0$.*

Proof. Since

$$A_k^n = \frac{[\omega(t_n)]^{-1}}{\Gamma(2-2\alpha)}\frac{[\sigma(t_n)-\sigma(t_{k-1})]^{1-2\alpha}-[\sigma(t_n)-\sigma(t_k)]^{1-2\alpha}}{[\sigma(t_k)-\sigma(t_{k-1})]}, \quad 1 \le k \le n.$$

So, for any $\omega(t) > 0$ and $t_k > t_{k-1}$, we have $\sigma(t_k) > \sigma(t_{k-1})$ as $\sigma(t) > 0$ is strictly increasing function, which implies that $\sigma(t_k) - \sigma(t_{k-1}) > 0$, and $[\sigma(t_n) - \sigma(t_{k-1})]^{1-2\alpha} > [\sigma(t_n) - \sigma(t_k)]^{1-2\alpha}$, and $\alpha \in [0, \frac{1}{2}]$. Hence, $A_k^n > 0$. Similarly, $B_k^n > 0$, $P_k^n > 0$, $Q_k^n > 0$. □

Error estimate of approximation

Here, we study the error estimate of approximation of the GFDs discussed in Section " Approximation of GFDs on non-uniform meshes".

Theorem 1. *For any* $\alpha \in [0, \frac{1}{2}]$, *and* $G(r) \in C^3[0, \sigma_n]$, *the following holds for approximation of first term in Eq. (7)*

$$|\hat{R}(G(r_1))| \leq \frac{\alpha 2^{2-2\alpha}}{\omega_1 \Gamma(3-\alpha)} \max_{\sigma_0 \leq \sigma \leq \sigma_1} |G''(r)| T^{2-2\alpha} (N+1)^{2\alpha-2}, \quad n = 1,$$

$$\begin{aligned}|\hat{R}(G(r_n))| \leq & \frac{2\alpha}{\omega_n \Gamma(1-\alpha)} \Big\{ \frac{2}{3} \max_{\sigma_0 \leq \sigma \leq \sigma_1} |G''(r)| T^{2-2\alpha} (N+1)^{2\alpha-2} \\ & + \Big[\frac{2}{3} \frac{(2\alpha+1)}{\alpha} + \frac{2^{3-2\alpha}}{6} \frac{1}{(2-2\alpha)(2-2\alpha)} \Big(\frac{2}{2-2\alpha} + 1 \Big) \Big] \\ & \times \max_{\sigma_0 \leq \sigma \leq \sigma_n} |G'''(r)| T^{3-2\alpha} (N+1)^{2\alpha-3} \Big\}, \quad n \geq 2.\end{aligned}$$

Proof. To analyze the error estimate of approximation, we assume $G(s) = \nu(s)\omega(s)$, and $r = \sigma(s)$, which implies $s = \sigma^{-1}(r)$, and $G(r) = \omega(\sigma^{-1}(r))\nu(\sigma^{-1}(r))$. □

For $n = 1$, we interpolate $G(r)$ on $[\sigma_0, \sigma_1]$ by linear interpolation polynomial $p_k^1(r)$ defined using points (σ_0, G_0) and (σ_1, G_1), i.e.,

$$G(r) - p_k^1(r) = \frac{G''(\xi_1)}{2!}(r-\sigma_0)(r-\sigma_1), \qquad \xi_1 \in [\sigma_0, \sigma_1]. \tag{25}$$

Thus, the truncation error for linear approximation of the first term of Eq. (7) is given by

$$\begin{aligned}|\hat{R}(G(r_1))| &= \frac{[\omega_1]^{-1}}{\Gamma(1-2\alpha)} \int_{\sigma_0}^{\sigma_1} [G(r) - p_k^1(r)]'(\sigma_1 - r)^{-2\alpha} dr, \\ &= \frac{[\omega_1]^{-1}}{\Gamma(1-2\alpha)} \int_{\sigma_0}^{\sigma_1} (\sigma_1 - r)^{-2\alpha} d[G(r) - p_k^1(r)], \\ &= \frac{[\omega_1]^{-1}}{\Gamma(1-2\alpha)} \Big\{ [G(r) - p_k^1(r)](\sigma_1 - r)^{-2\alpha}|_{r=\sigma_0}^{\sigma_1} \\ &\quad - 2\alpha \int_{\sigma_0}^{\sigma_1} [G(r) - p_k^1(r)](\sigma_1 - r)^{-2\alpha-1} dr \Big\}, \\ &= \frac{[\omega_1]^{-1}}{\Gamma(1-2\alpha)} \Big\{ -\frac{1}{2} G''(\xi_1)(r-\sigma_0)(\sigma_1 - r)^{1-2\alpha}|_{r=\sigma_0}^{\sigma_1} \\ &\quad + 2\alpha \int_{\sigma_0}^{\sigma_1} \frac{1}{2} G''(\xi_1)(r-\sigma_0)(\sigma_1 - r)^{-2\alpha} dr \Big\}, \\ &= \frac{\alpha[\omega_1]^{-1}}{2\Gamma(1-2\alpha)} G''(\eta_1) \int_{\sigma_0}^{\sigma_1} (r-\sigma_0)(\sigma_1 - r)^{-2\alpha} dr, \\ &= \frac{\alpha[\omega_1]^{-1}}{2\Gamma(3-2\alpha)} G''(\eta_1)(\sigma_1 - \sigma_0)^{2-2\alpha} = \frac{\alpha[\omega_1]^{-1}}{2\Gamma(3-2\alpha)} G''(\eta_1)\tau_1^{2-2\alpha}, \\ &= \frac{\alpha 2^{1-2\alpha}[\omega_1]^{-1}}{\Gamma(3-2\alpha)} G''(\eta_1) T^{2-2\alpha}(N+1)^{2\alpha-2}, \quad \eta_1 \in (\sigma_0, \sigma_1).\end{aligned} \tag{26}$$

For $n \geq 2$, we interpolate $G(r)$ on $[\sigma_{k-1}, \sigma_k]$ by quadratic interpolation polynomial $p_k^2(r)$ defined using points (σ_{k-2}, G_{k-2}), (σ_{k-1}, G_{k-1}), and (σ_k, G_k), i.e.,

$$G(r) - p_k^2(r) = \frac{G'''(\xi_k)}{3!}(r-\sigma_{k-2})(r-\sigma_{k-1})(r-\sigma_k), \ \ \xi_k \in [\sigma_{k-2}, \sigma_k], 2 \leq k \leq n. \tag{27}$$

Thus, the truncation error for quadratic approximation of the first term of Eq. (7) is given by

$|\hat{R}(G(r_n))|$

$$= \frac{[\omega_n]^{-1}}{\Gamma(1-2\alpha)}\Big[\int_{\sigma_0}^{\sigma_1}[G(r)-p_k^1(r)]'(\sigma_n-r)^{-2\alpha}dr + \sum_{k=2}^{n}\int_{\sigma_{k-1}}^{\sigma_k}[G(r)-p_k^2(r)]'(\sigma_n-r)^{-2\alpha}dr\Big],$$

$$= \frac{[\omega_n]^{-1}}{\Gamma(1-2\alpha)}\Big\{[G(r)-p_k^1(r)](\sigma_n-r)^{-2\alpha}|_{r=\sigma_0}^{\sigma_1} - 2\alpha\int_{\sigma_0}^{\sigma_1}[G(r)-p_k^1(r)] \times(\sigma_n-r)^{-2\alpha-1}dr + \sum_{k=2}^{n}\Big[[G(r)-p_k^2(r)](\sigma_n-r)^{-2\alpha}|_{r=\sigma_{k-1}}^{\sigma_k} - 2\alpha\int_{\sigma_{k-1}}^{\sigma_k}[G(r)-p_k^2(r)](\sigma_n-r)^{-2\alpha-1}dr\Big]\Big\},$$

$$= \frac{-2\alpha[\omega_n]^{-1}}{\Gamma(1-2\alpha)}\Big\{\int_{\sigma_0}^{\sigma_1}[G(r)-p_k^1(r)](\sigma_n-r)^{-2\alpha-1}dr + \sum_{k=2}^{n}\int_{\sigma_{k-1}}^{\sigma_k}[G(r)-p_k^2(r)](\sigma_n-r)^{-2\alpha-1}dr\Big\}. \tag{28}$$

From Eq. (27), it results

$$[G(r)-p_k^2(r)][\sigma_n-r]^{-2\alpha}|_{r=\sigma_{n-1}}^{\sigma_n} = \frac{G'''(\varphi_n)}{3!}(r-\sigma_{n-2})(r-\sigma_{n-1})(r-\sigma_n)(\sigma_n-r)^{-2\alpha}|_{r=\sigma_{n-1}}^{\sigma_n},$$
$$= -\frac{G'''(\varphi_n)}{3!}(r-\sigma_{n-2})(r-\sigma_{n-1})(\sigma_n-r)^{1-2\alpha}|_{r=\sigma_{n-1}}^{\sigma_n} = 0,$$

also from Eq. (25), it results

$$\Big|\int_{\sigma_0}^{\sigma_1}[G(r)-p_k^1(r)](\sigma_n-r)^{-2\alpha-1}dr\Big| = \Big|\int_{\sigma_0}^{\sigma_1}\frac{G''(\xi_1)}{2}(r-\sigma_0)(r-\sigma_1)(\sigma_n-r)^{-1-2\alpha}dr\Big|,$$
$$= \Big|\frac{G''(\eta_1)}{2}\int_{\sigma_1}^{\sigma_0}(r-\sigma_0)(\sigma_1-r)(\sigma_n-r)^{-1-2\alpha}dr\Big|,$$
$$\le \frac{1}{12}|G''(\eta_1)|(\sigma_n-\sigma_1)^{-1-2\alpha}\tau_1^3, \quad \eta_1\in(\sigma_0,\sigma_1). \tag{29}$$

The concept of non-uniform mesh (11) implies that

$$\sigma_n-\sigma_1 = \sum_{m=2}^{n}\tau_m = \frac{1}{2}(\tau_n+\tau_2)(n-1) = \frac{\mu}{2}(n-1)(2N-n),$$

thus,

$$\tau_1^3(\sigma_n-\sigma_1)^{-2\alpha-1} = 2^{1+2\alpha}\mu^{2-\alpha}(n-1)^{-\alpha-1}(2N-n)^{-2\alpha-1}N^3,$$
$$\le 2^{1+2\alpha}\mu^{2-2\alpha}(n-1)^{-2\alpha-1}(n-1)^{-1-2\alpha}N^{2-2\alpha}. \tag{30}$$

Notice that, for $n\ge 2$, $(n-1)^{-1-2\alpha}\le 1$. Then, we can write Eq. (30) as follows

$$\tau_1^3(\sigma_n-\sigma_1)^{-2\alpha-1} \le 2^{1+2\alpha}\mu^{2-2\alpha}N^{2-2\alpha} = \frac{8T^{2-2\alpha}}{(N+1)^{2-2\alpha}}. \tag{31}$$

From Eqs. (29) and (31), we obtain

$$\Big|\int_{\sigma_0}^{\sigma_1}[G(r)-p_k^1(r)](\sigma_n-r)^{-2\alpha-1}dr\Big| \le \frac{2}{3}|G''(\eta_1)|T^{2-2\alpha}(N+1)^{2\alpha-2}. \tag{32}$$

Noting that

$$\begin{aligned}
&\left|\sum_{k=2}^{n-1}\int_{\sigma_{k-1}}^{\sigma_k}[G(r)-p_k^2(r)](\sigma_n-r)^{-2\alpha-1}dr\right| \\
&\quad=\left|\sum_{k=2}^{n-1}\int_{\sigma_{k-1}}^{\sigma_k}\frac{G'''(\varphi_n)}{3!}(r-\sigma_{k-2})(r-\sigma_{k-1})(r-\sigma_k)(\sigma_n-r)^{-\alpha-1}dr\right|, \\
&\quad=\frac{1}{6}|G'''(\eta)|\sum_{k=2}^{n-1}\int_{\sigma_{k-1}}^{\sigma_k}(\sigma_n-r)^{-2\alpha-1}(r-\sigma_{k-2})(r-\sigma_{k-1})(r-\sigma_k)dr, \\
&\quad\le\frac{1}{24}|G'''(\eta)|\sum_{k=2}^{n-1}\tau_k^2(\tau_{k-1}+\tau_k)\int_{\sigma_{k-1}}^{\sigma_k}(\sigma_n-r)^{-2\alpha-1}dr, \qquad (33) \\
&\quad\le\frac{1}{24}|G'''(\eta)|\sum_{k=2}^{n-1}(\sigma_n-\sigma_k)^{-2\alpha-1}\tau_k^3(\tau_{k-1}+\tau_k), \qquad (34)
\end{aligned}$$

where $\eta\in(\sigma_0,\sigma_{k-1})$, $2\le k\le n-1$. Equation (33) is the result of the following remark:

Remark 1. The $\max_{\sigma_0\le r\le\sigma_n}|(r-\sigma_k)(r-\sigma_{k-1})|=\frac{\tau_k^4}{4}$ is obtained at $r=\sigma_{k-1}+\frac{\tau_k}{2}$, then we have:

$$(r-\sigma_k)(r-\sigma_{k-1})(r-\sigma_{k-2})=\frac{\tau_k^2}{4}(\sigma_{k-1}+\frac{\tau_k}{2}-\sigma_{k-2})\le\frac{\tau_k^2}{4}(\tau_{k-1}+\tau_k).$$

Also, from the definition of non-uniform mesh (11), we conclude

$$\sigma_n-\sigma_k=\sum_{m=k+1}^{n}\tau_m=\frac{1}{2}(\tau_n+\tau_{k+1})(n-k)=\frac{\mu}{2}(2N-n-k+1)(n-k),$$

and also

$$\begin{aligned}
&\sum_{k=2}^{n-1}(\sigma_n-\sigma_k)^{-2\alpha-1}\tau_k^3(\tau_{k-1}+\tau_k) \\
&\quad=2^{1+2\alpha}\mu^{3-2\alpha}\sum_{k=2}^{n-1}(N-k+1)^3(2N-2k+3)(n-k)^{-2\alpha-1} \\
&\quad\times(2N-n-k+1)^{-2\alpha-1}, \\
&\quad\le 2^{2+2\alpha}\mu^{3-2\alpha}\sum_{k=2}^{n-1}(n-k)^{-2\alpha-1}(N-k+1)^3(N-k+\frac{3}{2}), \\
&\quad\le 2^{2+2\alpha}N^{3-2\alpha}\mu^{3-2\alpha}\sum_{k=2}^{n-1}(n-k)^{-2\alpha-1}, \\
&\quad=32T^{3-2\alpha}(N+1)^{2\alpha-3}\sum_{k=2}^{n-1}(n-k)^{-2\alpha-1}.
\end{aligned}$$

Since, $\sum_{k=2}^{n-1}(n-k)^{-2\alpha-1}\le 1+\frac{1}{2\alpha}$, we get

$$\begin{aligned}
&\left|\sum_{k=2}^{n-1}\int_{\sigma_{k-1}}^{\sigma_k}[G(r)-p_k^2(r)](\sigma_n-r)^{-2\alpha-1}dr\right| \\
&\quad\le\frac{2}{3}\frac{(2\alpha+1)}{\alpha}|G'''(\eta)|T^{3-2\alpha}(N+1)^{2\alpha-3}. \qquad (35)
\end{aligned}$$

In addition,

$$\begin{aligned}
&\left|\int_{\sigma_{n-1}}^{\sigma_n}[G(r)-p_k^2(r)](\sigma_n-r)^{-2\alpha-1}dr\right| \\
&=\left|\int_{\sigma_{n-1}}^{\sigma_n}\frac{G'''(\varphi_n)}{3!}(r-\sigma_{n-2})(r-\sigma_{n-1})(r-\sigma_n)(\sigma_n-r)^{-2\alpha-1}dr\right|, \\
&=\left|\frac{-1}{6}G'''(\eta_n)\int_{\sigma_{n-1}}^{\sigma_n}(r-\sigma_{n-2})(r-\sigma_{n-1})(\sigma_n-r)^{-2\alpha}dr\right|, \\
&\le\frac{2^{3-2\alpha}}{6}\frac{1}{(1-2\alpha)(2-2\alpha)}\left[\left(\frac{2}{3-2\alpha}+1\right)T^{3-2\alpha}(N+1)^{2\alpha-3}\right]|G'''(\eta_n)|, \\
&\text{where, } \eta_n\in(\sigma_{n-1},\sigma_n). \qquad (36)
\end{aligned}$$

Theorem 2. *For any $0<\alpha<1$, and $G(r)\in C^3[0,\sigma_n]$, the following holds for the approximation of second term in Eq. (7)*

$$\begin{aligned}
|\hat{R}(G(r_1))| \le& \frac{\alpha 2^{1-\alpha}}{\omega_1\Gamma(3-\alpha)}\max_{\sigma_0\le\sigma\le\sigma_1}|G''(r)|T^{2-\alpha}(N+1)^{\alpha-2}, \quad n=1, \\
|\hat{R}(G(r_n))| \le& \frac{\alpha}{\omega_n\Gamma(1-\alpha)}\left\{\frac{2}{3}\max_{\sigma_0\le\sigma\le\sigma_1}|G''(r)|T^{2-\alpha}(N+1)^{\alpha-2}\right. \\
&+\left[\frac{2}{3}\frac{(\alpha+1)}{\alpha}+\frac{2^{3-\alpha}}{6}\frac{1}{(2-2\alpha)(3-2\alpha)}\left(\frac{2}{3-2\alpha}+1\right)\right] \\
&\left.\times\max_{\sigma_0\le\sigma\le\sigma_n}|G'''(r)|T^{3-\alpha}(N+1)^{\alpha-3}\right\}, \quad n\ge 2.
\end{aligned}$$

A fourth-order compact difference scheme

To discretize the classical second-order spatial derivative of $v(x,t)$, we use a fourth-order compact finite difference scheme [35,36]. Let $h=L/M, M\in\mathbb{N}^+$, for spatial approximation and $x_i=ih(0\le i\le M)$. For any grid function $y(x_i)=y_i$, the notations are defined as follows

$$\delta_x y_{i-\frac{1}{2}}=\frac{1}{h}[y_i-y_{i-1}], \qquad \delta_x^2 y_i=\frac{1}{h}[\delta_x y_{i+\frac{1}{2}}-\delta_x y_{i-\frac{1}{2}}],$$

$$\mathcal{H}y_i=\begin{cases}\frac{1}{12}(y_{i+1}+10y_i+y_{i-1}), & 1\le i\le M-1,\\ y_i & i=0 \text{ or } M.\end{cases}$$

It is clear that

$$\mathcal{H}y_i=\left(1+\frac{h^2}{12}\delta^2\right)y_i, \qquad 1\le i\le M-1.$$

Lemma 2. *(see [37])Let function $G(x)\in C^6[x_{i-1},x_{i+1}]$, and $\xi(s)=5(1-s)^3-3(1-s)^5$, then*

$$\begin{aligned}
&\frac{1}{12}(G''(x_{i+1})+10G''(x_i)+G''(x_{i-1}))=\frac{1}{h^2}(G(x_{i+1})-2G(x_i)+G(x_{i-1})) \\
&+\frac{h^4}{360}\int_0^1[G^6(x_i-sh)+G^6(x_i+sh)]\xi(s)ds.
\end{aligned}$$

We use the notations,

$$v_i^n=v(x_i,t_n), \quad f_i^n=f(x_i,t_n), \qquad 0\le i\le M, \quad 1\le n\le N.$$

Using the approximation of GFD obtained in Eq. (24), Eq. (7) takes the form,

$$\sum_{k=1}^{n}a_k^n(v_k\omega_k-v_{k-1}\omega_{k-1})=\kappa^2\frac{\partial^2 v}{\partial x^2}(x_i,t_n)+f_i^n+(R_t)_i^n,$$

$$1\le i\le M-1, \ \ 1\le n\le N. \qquad (1)$$

Applying the operator $\mathcal{H}$ on both side of Eq. (1), we get

$$\mathcal{H}\Big[\sum_{k=1}^{n} a_k^n(v_i^k\omega_k - v_i^{k-1}\omega_{k-1})\Big] = \kappa^2\mathcal{H}\frac{\partial^2 v}{\partial x^2}(x_i,t_n) + \mathcal{H}f_i^n + \mathcal{H}(R_t)_i^n. \tag{2}$$

Lemma 2 implies that

$$\mathcal{H}\frac{\partial^2 v}{\partial x^2}(x_i,t_n) = \delta_x^2 v_i^n + (R_x)_i^n, \quad 1 \le i \le M-1, \ 1 \le n \le N, \tag{3}$$

where,

$$(R_x)_i^n = \frac{h^4}{360}\int_0^1\Big[\frac{\partial^6 v}{\partial x^6}(x_i - sh) + \frac{\partial^6 v}{\partial x^6}(x_i + sh)\Big]\xi(s)ds.$$

Substituting (3) into (2), we obtain

$$\mathcal{H}\Big[\sum_{k=1}^{n} a_k^n(v_i^k\omega_k - v_i^{k-1}\omega_{k-1})\Big] = \kappa^2\delta_x^2 v_i^n + \mathcal{H}f_i^n + (R)_i^n,$$

where,

$$R_i^n = \mathcal{H}(R_t)_i^n + (R_x)_i^n. \tag{4}$$

It follows from non-uniform mesh (11) that

$$|R_i^n| \le C_R(N^{2\alpha-3} + h^4), \quad 1 \le i \le M-1, \ 1 \le n \le N, \tag{5}$$

where C_R is a positive constant.

By omitting the small term R_i^n, we get the following difference scheme

$$\mathcal{H}\Big[\sum_{k=1}^{n} a_k^n(v_i^k\omega_k - v_i^{k-1}\omega_{k-1})\Big] = \kappa^2\delta_x^2 v_i^n + \mathcal{H}f_i^n, \ 1 \le i \le M-1, \ 1 \le n \le N, \tag{6}$$

$$v_i^0 = \phi(x_i), \qquad 0 \le i \le M, \tag{7}$$

$$v_0^n = g_1(t_n), \quad v_m^n = g_2(t_n), \qquad 1 \le n \le N. \tag{8}$$

Matrix form

Matrix form of the above scheme can be obtained by writing Eq. (6) at each mesh point and $v^n = [v_1^n, v_2^n, \cdots, v_{M-1}^n]^T$

$$\begin{cases} D_1 v^1 = D_2 v^0 + F^1, & n = 1, \\ D_3 v^n = D_4 v^0 - \sum_{k=1}^{n} E_k^n v^k + F^n, & n = 2, 3, \cdots, N, \end{cases} \tag{9}$$

From Eq. (9), we define the triangular matrices as follows

$$D_1 = tri\Big[\frac{1}{12}a_1^1\omega_1 - \frac{\kappa^2}{h^2}, \frac{10}{12}a_1^1\omega_1 + \frac{2\kappa^2}{h^2}, \frac{1}{12}a_1^1\omega_1 - \frac{\kappa^2}{h^2}\Big]_{M-1\times M-1},$$

$$D_2 = tri\Big[\frac{1}{12}a_1^1\omega_0, \frac{10}{12}a_1^1\omega_0, \frac{1}{12}a_1^1\omega_0\Big]_{M-1\times M-1},$$

$$D_3 = tri\Big[\frac{1}{12}a_n^n\omega_n - \frac{\kappa}{h^2}, \frac{10}{12}a_n^n\omega_n + \frac{2\kappa^2}{h^2}, \frac{1}{12}a_n^n\omega_n - \frac{\kappa}{h^2}\Big]_{M-1\times M-1},$$

$$D_4 = tri\Big[\frac{1}{12}a_1^n\omega_0, \frac{10}{12}a_1^n\omega_0, \frac{1}{12}a_1^n\omega_0\Big]_{M-1\times M-1},$$

and the column vector F^n is given by

$$F^n = \begin{pmatrix} \mathcal{H}f_1^n - \left[\frac{1}{12}a_n^n\omega_n - \frac{\kappa^2}{h^2}\right]v_0^n \\ \mathcal{H}f_2^n \\ \vdots \\ \mathcal{H}f_{M-2}^n \\ \mathcal{H}f_{M-1}^n - \left[\frac{1}{12}a_n^n\omega_n - \frac{\kappa^2}{h^2}\right]v_M^n \end{pmatrix}, \quad 1 \le n \le N,$$

and

$$E_k^n = (a_{k+1}^n - a_k^n)\omega_k \begin{pmatrix} \frac{10}{12} & \frac{1}{12} & & & \\ \frac{1}{12} & \frac{10}{12} & \frac{1}{12} & & \\ & \ddots & \ddots & \ddots & \\ & & \frac{1}{12} & \frac{10}{12} & \frac{1}{12} \\ & & & \frac{1}{12} & \frac{10}{12} \end{pmatrix},$$

where a_k^n is defined in (24).

Stability and convergence analysis

The coefficient matrices D_1 and D_3 are strictly diagonal dominant for any possible values of τ_n, h, and α, and thus they are non-singular and invertible. As a result, the difference scheme (6)–(8) has a unique solution.

Stability

Let $\tilde{v}_n$ be another approximation of the scheme (6), and define

$$\varrho_i^n = v_i^n - \tilde{v}_i^n, \qquad 0 \le i \le M, \ 1 \le n \le N.$$

Suppose $\varrho^n = (\varrho_0^n, \varrho_1^n, \cdots, \varrho_M^n)$, and the infinity norm is defined as,

$$||\varrho^n||_\infty = \max_{0\le i\le M} |\varrho_i^n| = |\varrho_j^n|.$$

It follows from (6) that

$$a_n^n\mathcal{H}(v_i^n\omega_n - v_i^n\omega_{n-1}) + \sum_{k=1}^{n-1} a_k^n\mathcal{H}(v_i^k\omega_k - v_i^{k-1}\omega_{k-1}) = \kappa^2\delta_x^2 v_i^n + \mathcal{H}f_i^n$$

After simplification of terms, we have

$$\begin{aligned} &K_1v_{i+1}^n + K_2v_i^n + K_1v_{i-1}^n \\ &\qquad = \mathcal{H}v_i^{n-1}\omega_{n-1} - \frac{1}{a_n^n}\sum_{n}^{n} a_n^n\mathcal{H}(v_i^k\omega_k - v_i^{k-1}\omega_{k-1}) + \frac{1}{a_n^n}\mathcal{H}f_i^n, \\ &\qquad = \frac{1}{a_n^n}\sum_{k=0}^{n-1}(a_{k+1}^n - a_k^n)\mathcal{H}v_i^k\omega_k + \frac{1}{a_n^n}\mathcal{H}f_i^n, \end{aligned}$$

where $K_1 = \frac{1}{12}\omega_n - \frac{\kappa^2}{a_n^n h^2}$, $K_2 = \frac{10}{12}\omega_n + \frac{2\kappa^2}{a_n^n h^2}$.

So, the round-off error equation is as follows

$$\begin{aligned} &K_1\varrho_{i+1}^n + K_2\varrho_i^n + K_1\varrho_{i-1}^n \\ &\qquad = \frac{1}{a_n^n}\sum_{k=0}^{n-1}(a_{k+1}^n - a_k^n)\omega_k\left(\frac{1}{12}\varrho_{i+1}^k + \frac{10}{12}\varrho_i^k + \frac{1}{12}\varrho_{i-1}^k\right). \end{aligned} \tag{1}$$

For simplicity in our further calculation, we define

$$L_1\varrho_i^n = K_1\varrho_{i+1}^n + K_2\varrho_i^n + K_1\varrho_{i-1}^n \tag{2}$$

$$L_2\varrho_i^{n-1} = \frac{1}{a_n^n}\sum_{k=0}^{n-1}(a_{k+1}^n - a_k^n)\omega_k\left(\frac{1}{12}\varrho_{i+1}^k + \frac{10}{12}\varrho_i^k + \frac{1}{12}\varrho_{i-1}^k\right) \tag{3}$$

Now, Eq. (1) can be rewritten as follows

$$L_1\varrho_i^n = L_2\varrho_i^{n-1}.$$

From Eq. (3), we obtain

$$\begin{aligned}|L_2\varrho_i^{n-1}| &= \left|\frac{1}{a_n^n}\sum_{k=0}^{n-1}(a_{k+1}^n - a_k^n)\omega_k\left(\frac{1}{12}\varrho_{i+1}^k + \frac{10}{12}\varrho_i^k + \frac{1}{12}\varrho_{i-1}^k\right)\right|,\\ &= \frac{1}{a_n^n}\left(|\frac{1}{12}\varrho_{i+1}^{n-1}| + |\frac{10}{12}\varrho_i^{n-1}| + |\frac{1}{12}\varrho_{i-1}^{n-1}|\right)|\sum_{k=0}^{n-1}(a_{k+1}^n - a_k^n)|,\end{aligned}$$

where $|\varrho_i^{n-1}| = \max_{0\le k\le n-1}|\varrho_i^k|$. But, since $|\sum_{k=0}^{n-1}(a_{k+1}^n - a_k^n)| = a_n^n$ and noting that $a_0^n > 0$ and $a_n^n > 0$,

$$|L_2\varrho_i^n| \le |\frac{1}{12}\varrho_{i+1}^{n-1}| + |\frac{10}{12}\varrho_i^{n-1}| + |\frac{1}{12}\varrho_{i-1}^{n-1}|. \tag{4}$$

Thus, from Eqs. (2), (3) and (4), we conclude that

$$\begin{aligned}||\varrho^n||_\infty &= |\varrho_j^n| = |K_1\varrho_j^n + K_2\varrho_j^n + K_1\varrho_j^n|\\ &= |L_1\varrho_j^n| = |L_2\varrho_j^n| \le |\varrho_j^{n-1}| = ||\varrho^{n-1}||_\infty\end{aligned}$$

i.e.,

$$||\varrho^n||_\infty \le ||\varrho^0||_\infty, \quad 1 \le n \le N.$$

This means that the scheme proposed in this paper is unconditionally stable.

Convergence

Let v_i^n be the numerical solution of scheme (6)–(8) and $v(x,t)$ be the exact solution of Eq. (7). Let the error at (x_i, t_n) be

$$\mathcal{E}(x_i,t_n) = v(x_i,t_n) - v_i^n, \qquad 0 \le i \le M,\ 1 \le n \le N.$$

Then, the error term of (6)–(8) will be

$$\begin{aligned}&L_1\mathcal{E}_i^n = L_2\mathcal{E}_i^{n-1} + R_i^n, \qquad 0 \le i \le M,\ 1 \le n \le N\\ &\mathcal{E}_0^n = \mathcal{E}_M^n = 0, \qquad 1 \le n \le N\\ &\mathcal{E}_i^0 = 0, \qquad 0 \le i \le M.\end{aligned}$$

We define

$$||\mathcal{E}^n||_\infty = \max_{0\le i\le M}|\mathcal{E}_i^n| = |\mathcal{E}_j^n|,$$

then, we obtain

$$\begin{aligned}||\mathcal{E}^n||_\infty &= |\mathcal{E}_j^n| = |L_1\mathcal{E}_j^n| = |L_2\mathcal{E}_j^{n-1} + R_j^n|\\ &\le |L_2\mathcal{E}_j^{n-1}| + |R_j^n| \le |\mathcal{E}_j^{n-1}| + |R_j^n| \le ||\mathcal{E}^{n-1}||_\infty + |R_{\max}|,\end{aligned}$$

where $R_{\max} = max_{n,j}|R_j^n|$.

Table 1
(Example 1) MAE and CO for $\sigma(t) = t$, $\omega(t) = 1$ and different values of α.

	$\alpha = 0.2$		$\alpha = 0.3$		$\alpha = 0.4$	
N	MAE	CO	MAE	CO	MAE	CO
10	1.4321e-2		3.6581e-2		8.4012e-2	
20	2.6410e-3	2.4389	7.4836e-3	2.2893	1.9466e-2	2.1096
40	4.6396e-4	2.5090	1.4722e-3	2.3457	4.3275e-3	2.1694
80	7.9282e-5	2.5489	2.8345e-4	2.3768	9.4902e-4	2.1890
160	1.3342e-5	2.5710	5.3947e-5	2.3935	2.0646e-4	2.2005

Table 2
(Example 1) MAE and CO for $\alpha = 0.3$, $\sigma(t) = t$ and different values of weight function $\omega(t)$.

	$\omega(t) = e^t$		$\omega(t) = e^{4t}$		$\omega(t) = t + 1$	
N	MAE	CO	MAE	CO	MAE	CO
10	6.2187e-2		1.8424e-1		4.9029e-2	
20	1.3252e-2	2.2304	4.3525e-2	2.0817	1.0515e-2	2.2211
40	2.6682e-3	2.3123	9.2943e-3	2.2274	2.0985e-3	2.3251
80	5.2023e-4	2.3586	2.3101e-3	2.3101	4.0754e-4	2.3643
160	9.9773e-5	2.3824	3.6627e-4	2.3552	7.7974e-5	2.3859

For $n = 1$, we have

$$||\mathcal{E}^1||_\infty \leq ||\mathcal{E}^0||_\infty + R_{\max} = R_{\max}.$$

Then

$$||\mathcal{E}^n||_\infty \leq R_{\max}, \qquad 1 \leq n \leq N.$$

Numerical results

Here, we discuss four numerical examples to verify the accuracy of our scheme on the non-uniform meshes. The first example verifies the convergence of the scheme (24) for approximating GFD. The next three examples validate the performance of the scheme (6) for the GFTE on non-uniform meshes.

Let v_i^N be the numerical solution and V_i^N be the exact solution of the problem taken in this paper. We use the following formula to calculate the maximum absolute error (MAE) and convergence order (CO) of the presented numerical scheme

$$e(M,N) = \max_{0\leq i\leq M-1} |V_i^N - v_i^N|, \qquad CO = log_2\left(\frac{e(M/2,N)}{e(M,N)}\right).$$

Example 1. Consider the function $f(t) = t^{4+\alpha}$, $\alpha \in (0, \frac{1}{2}]$. For $\sigma(t) = t$ and $\omega(t) = 1$, the exact solution is given by Gao et al. [33]

$$({}^*\mathbb{D}^{2\alpha} + 2\beta\,{}^*\mathbb{D}^{\alpha})t^{4+\alpha} = \frac{\Gamma(5+\alpha)}{\Gamma(5-\alpha)}t^{4-\alpha} + 2\beta\frac{\Gamma(5+\alpha)}{24}t^4. \tag{5}$$

Taking different temporal sizes, MAE and CO are obtained in calculating GFD of function $f(t) = t^{4+\alpha}$ using scheme (24).Table 1–3 represents the MAE and CO for different choices of $\alpha, \omega(t), \sigma(t)$. From Table 1, we see that the temporal convergence is approximately $O(N^{2\alpha-3})$ for different α. In Table 2, we fix $\sigma(t) = t$ and take $\omega(t) = e^t, e^{2t}$ and $t + 1$. The scheme yields $O(N^{2\alpha-3})$ convergence in all cases. Table 3 represents the convergence rate of $O(N^{2\alpha-2})$ for non-linear scale function $\sigma(t) = t^2, t^{0.8}$, while $O(N^{2\alpha-3})$ for linear scale function $\sigma(t) = 10t$.

Table 3
(Example 1) MAE and CO for $\alpha = 0.3$, $\omega(t) = 1$ and different values of scale function $\sigma(t)$.

	$\sigma(t) = t^2$		$\sigma(t) = t^{0.8}$		$\sigma(t) = 10t$	
N	MAE	CO	MAE	CO	MAE	CO
10	2.0437e-2		2.2773e-1		1.0108e-2	
20	1.1083e-2	0.8828	6.9924e-2	1.7180	2.0429e-3	2.3068
40	4.9924e-3	1.1506	2.2814e-2	1.6014	3.9694e-4	2.3636
80	2.0543e-3	1.2811	7.9894e-3	1.5138	7.5511e-5	2.3942
160	8.1509e-4	1.3336	2.8688e-3	1.4776	1.3935e-5	2.4379

Table 4
(Example 2) MAE and CO for $\alpha = 0.2, \beta = 1, \kappa^2 = 1, \sigma(t) = t, \omega(t) = 1$.

		Our Scheme			Kumar et al. [30]	
M	N	MAE	CO	Time(s)	MAE	CO
10	10	2.4048e-5		0.038806	2.9303e-4	
20	20	3.6142e-6	2.7342	0.044867	9.5736e-5	1.6139
40	40	5.3161e-7	2.7652	0.085281	3.1143e-5	1.6201
80	80	7.7844e-8	2.7717	0.371392	1.0090e-5	1.6259
160	160	1.1454e-8	2.7647	3.424855	3.2606e-6	1.6298

Table 5
(Example 2) MAE and CO for $\alpha = 0.4, \beta = 1, \kappa^2 = 1, \sigma(t) = t, \omega(t) = 1$.

		Our Scheme			Kumar et al. [30]	
M	N	MAE	CO	Time(s)	MAE	CO
10	10	9.0570e-5		0.063490	1.4280e-3	
20	20	1.7229e-5	2.3942	0.077925	5.8646e-4	1.2839
40	40	3.3826e-6	2.3486	0.139176	2.4321e-4	1.2698
80	80	6.8360e-7	2.3069	0.598409	1.0168e-4	1.2582
160	160	1.4130e-7	2.2744	3.708309	4.2821e-5	1.2477

Example 2. Consider the following GFTE

$$\begin{cases} \frac{{}^*\partial^{2\alpha} v(x,t)}{{}^*\partial t^{2\alpha}} + 2\beta \frac{{}^*\partial^{\alpha} v(x,t)}{{}^*\partial t^{\alpha}} = \kappa^2 \frac{\partial^2 v(x,t)}{\partial x^2} + f(x,t), \\ v(x,0) = 0, \quad 0 \le x \le 1, \\ v(0,t) = 0, \ v(1,t) = 0, \quad t > 0, \end{cases} \tag{6}$$

where $f(x,t) = \frac{2x(x-1)t^{2-2\alpha}}{\Gamma(3-2\alpha)} + \frac{4\beta x(x-1)t^{2-\alpha}}{\Gamma(3-\alpha)} - 2\kappa^2 t^2$. The exact solution of Eq. (6) is $v(x,t) = x(x-1)t^2$ for $\omega(t) = 1$ and $\sigma(t) = t$.

MAE and CO are computed for various step sizes in Example 2. Tables 4 and 5 show that the numerical convergence of our scheme order is $O(N^{2\alpha-3})$, which is a better convergence than the scheme described in Kumar et al. [30]. Also, Tables 4 and 5 demonstrate the CPU time of our scheme. Figure 1 exhibits the plot of absolute error for different values of α.

Example 3. Consider the following GFTE

$$\begin{cases} \frac{{}^*\partial^{2\alpha} v(x,t)}{{}^*\partial t^{2\alpha}} + 2\beta \frac{{}^*\partial^{\alpha} v(x,t)}{{}^*\partial t^{\alpha}} = \kappa^2 \frac{\partial^2 v(x,t)}{\partial x^2} + f(x,t), \\ v(x,0) = sin(2\pi x), \quad 0 \le x \le 1, \\ v(0,t) = 0, \ v(1,t) = 0, \quad t > 0, \end{cases} \tag{7}$$

where $f(x,t) = \frac{2x(x-1)t^{2-2\alpha}}{\Gamma(3-2\alpha)} + \frac{4\beta x(x-1)t^{2-\alpha}}{\Gamma(3-\alpha)} + 4\kappa^2\pi^2 \sin(2\pi x) - 2\kappa^2 t^2$. The exact solution of Eq. (7) is $v(x,t) = x(x-1)t^2 + sin(2\pi x)$ for $\omega(t) = 1$ and $\sigma(t) = t$.

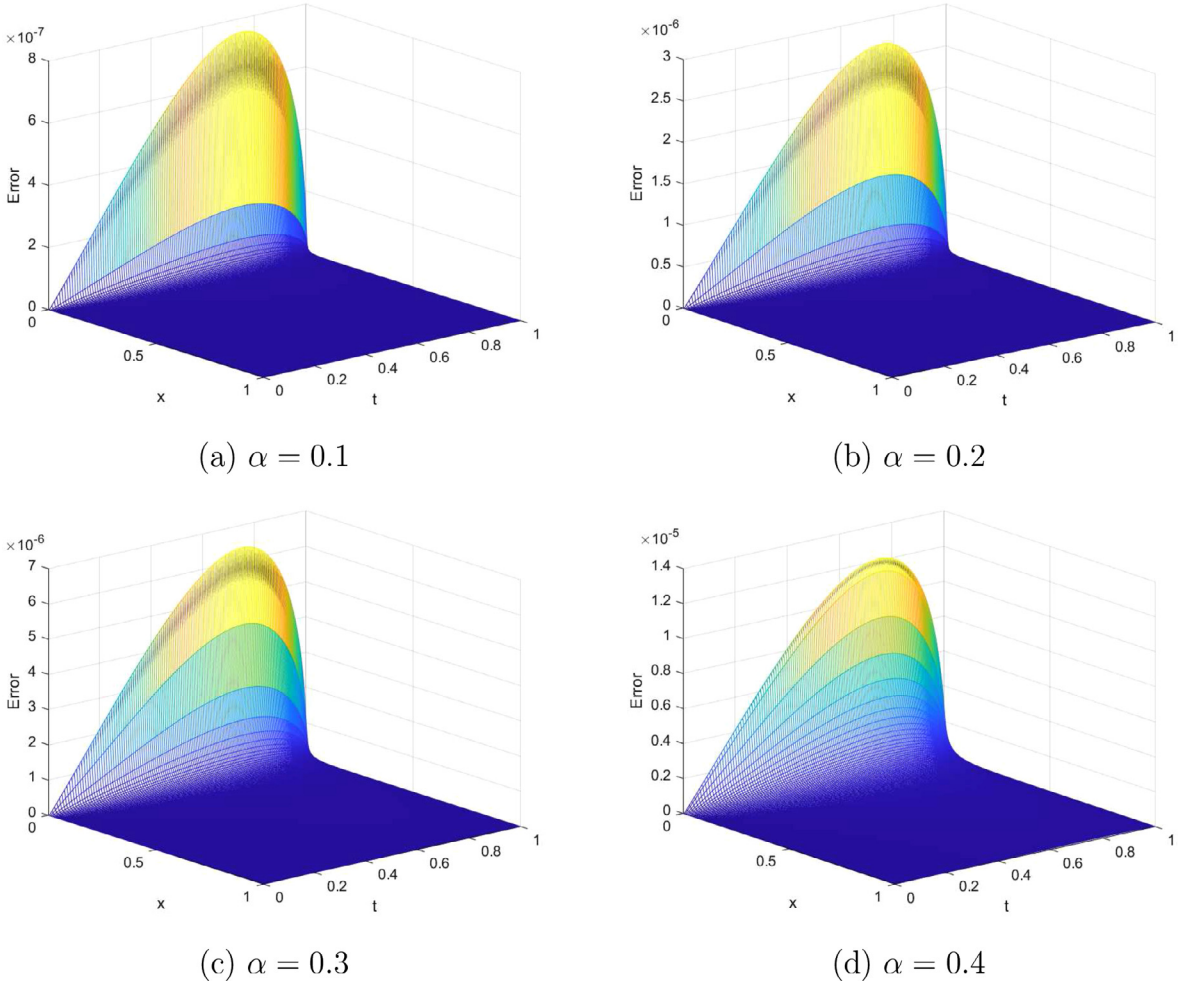

Fig. 1. (Example 2) Absolute error plot with $\sigma(t) = t$, $\omega(t) = 1$, $M = N = 200$, and for different values of order α..

Table 6
(Example 3) MAE and CO for $\alpha = 0.4, \beta = 1, \kappa^2 = 1, \sigma(t) = t, \omega(t) = 1$.

		Our Scheme			Kumar et al. [30]	
M	N	MAE	CO	Time(s)	MAE	CO
10	10	6.7440e-4		0.041328	1.4280e-3	
20	20	5.1187e-5	3.7198	0.052798	5.8646e-4	1.2839
40	40	5.0267e-6	3.3481	0.093309	2.4321e-4	1.2698
80	80	7.3242e-7	2.7789	0.379601	1.0168e-4	1.2582
160	160	1.4067e-7	2.3803	2.362974	4.2821e-5	1.2477

Table 7
(Example 3) MAE and CO in temporal direction with $\alpha = 0.4, \beta = 1, \kappa^2 = 1, M = 1000, \sigma(t) = t, \omega(t) = 1$.

	$\alpha = 0.1$		$\alpha = 0.4$		$\alpha = 0.4$ [30]	
N	MAE	CO	MAE	CO	MAE	CO
10	8.9650e-5		8.9650e-5		1.4189e-3	
20	1.7046e-5	2.3949	1.7046e-5	2.3949	5.8555e-4	1.2769
40	3.3436e-6	2.3499	3.3436e-6	2.3499	2.4320e-4	1.2677
80	6.7505e-7	2.3083	6.7505e-7	2.3083	1.0187e-4	1.2554
160	1.3940e-7	2.2758	1.3940e-7	2.2758	4.3288e-5	1.2347

Table 8
(Example 3) MAE and CO in spatial direction with $\alpha = 0.4, \beta = 1, \kappa^2 = 1, N = 1000, \sigma(t) = t, \omega(t) = 1$.

	$\alpha = 0.1$		$\alpha = 0.4$		$\alpha = 0.4$ [30]	
M	MAE	CO	MAE	CO	MAE	CO
10	5.8672e-4		6.0261e-4		3.0616e-2	
20	3.8105e-5	3.9446	3.9138e-5	3.9446	7.9392e-3	1.9472
40	2.3746e-6	4.0042	2.4404e-6	4.0033	1.9804e-3	2.0032
80	1.4831e-7	4.0010	1.5394e-7	3.9867	4.9706e-4	1.9943
160	9.2784e-9	3.9986	1.1175e-8	3.7840	1.2663e-4	1.9728

In Example 3, MAE and CO are calculated for different values of step sizes.Tables 6–8 show that our scheme gives better convergence than the scheme presented in Kumar et al. [30] in both temporal and spatial directions. Tables 7 and 8 verify the theoretical convergence of $O(N^{2\alpha-3})$ in the temporal direction and 4 in the spatial direction, respectively. Fig. 2 exhibits the absolute error plot with $M = N = 20, x = 0.5, \omega(t) = 1, \sigma(t) = t$ and for different value of α.

Example 4. Consider the following GFTE

$$\begin{cases} \frac{{}^{*}\partial^{2\alpha} v(x,t)}{{}^{*}\partial t^{2\alpha}} + 2\beta \frac{{}^{*}\partial^{\alpha} v(x,t)}{{}^{*}\partial t^{\alpha}} = \kappa^2 \frac{\partial^2 v(x,t)}{\partial x^2} + f(x,t), \\ v(x,0) = 0, \quad 0 \le x \le 1, \\ v(0,t) = t^5, \ \ v(1,t) = et^5, \quad t > 0, \end{cases} \tag{8}$$

where $f(x,t) = \frac{120e^x t^{5-2\alpha}}{\Gamma(6-2\alpha)} - \frac{240\beta e^x t^{5-\alpha}}{\Gamma(6-\alpha)} - t^5 e^x$. The exact solution of Eq. (8) is $v(x,t) = e^x t^5$ for $\omega(t) = 1$ and $\sigma(t) = t$.

In Example 4, we study the effect of different step sizes, $\omega(t)$ and $\sigma(t)$ on the numerical solution graphically. Figure 3 depict the exact solution to Eq. (8) with $\omega(t) = 1, \sigma(t) = t$, while Figs. 4–6 depicts the numerical solution for $\omega(t) = 1, \sigma(t) = t$. From Figs. 4–6, the following observation can be drawn.

Figure 4 shows that as the step size is reduced, the numerical solution surface becomes smooth, which indicates that the scheme presented in this study is stable.

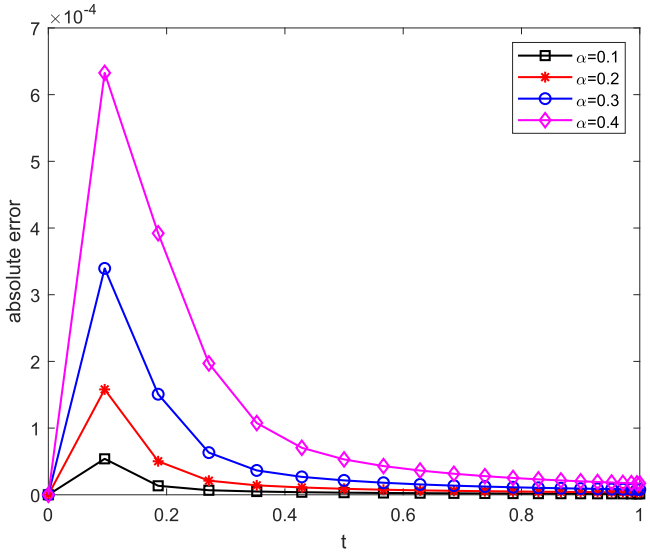

Fig. 2. (Example 3) Error plot for different values of α.

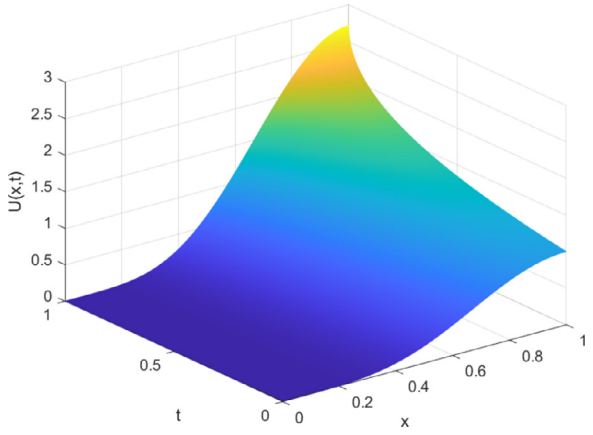

Fig. 3. (Example 4) Exact solution.

From Fig. 5, we examine the effect of increasing and decreasing weight functions on the solution of GFTE.

- From Fig. 5(a) and (b), we see that for increasing weight function $\omega(t) = e^{2t}, e^{4t}$, the solution shifts in the upward direction.
- From Fig. 5(c) and (d), we observe that for decreasing weight function $\omega(t) = e^{-2t}, e^{-4t}$, the solution shifts in the downward direction.

Hence, from Fig. 5, we conclude that the behaviour of the weight function has a direct impact on the numerical solution of the GFTE.

Fig. 6 shows the influence of contracting and stretching scale functions on the solutions of GFTE.

- From Fig. 6(a) and (b), we see that for the contracting scale function $\sigma(t) = t^2, t^5$, the solution's behavior is stretching.

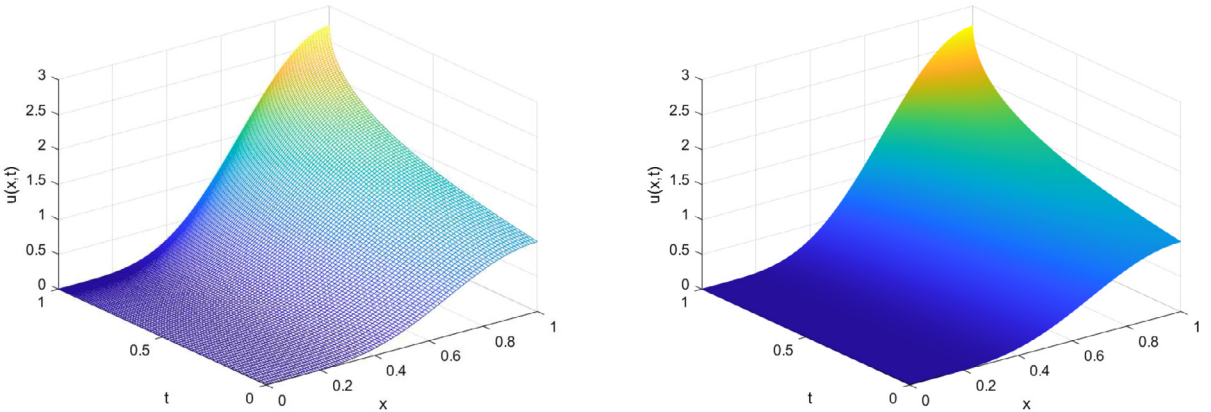

(a) $\alpha = 0.3,\ M = N = 100$ (b) $\alpha = 0.3,\ M = N = 500$

Fig. 4. (Example 4) Numerical solution for $\alpha = 0.3$, $\sigma(t) = t$, $\omega(t) = 1$ and different values of step sizes.

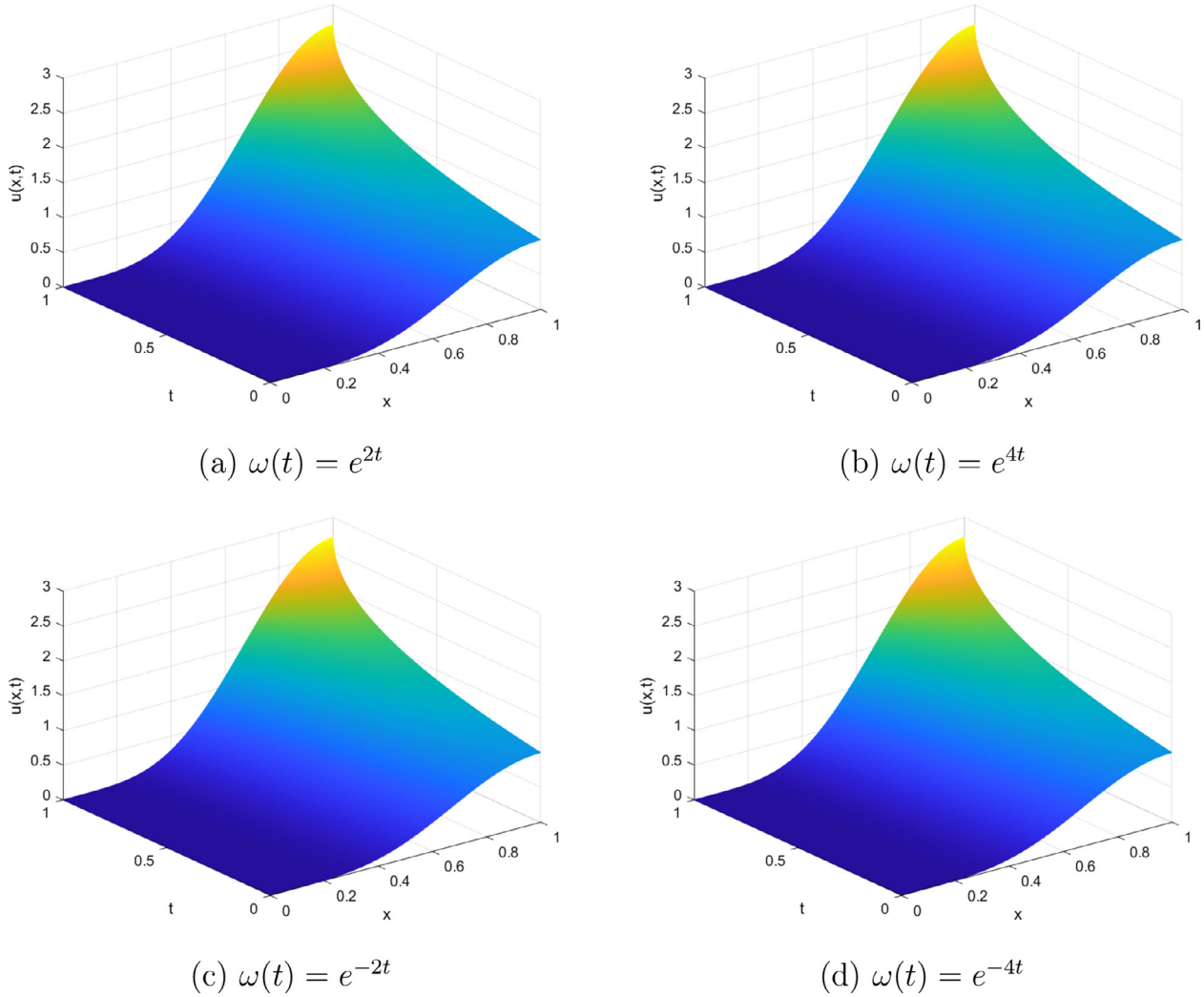

Fig. 5. (Example 4) Numerical solution for fixed step sizes $M = N = 500$, $\alpha = 0.3$, $\sigma(t) = t$ and different values of weight function $\omega(t)$.

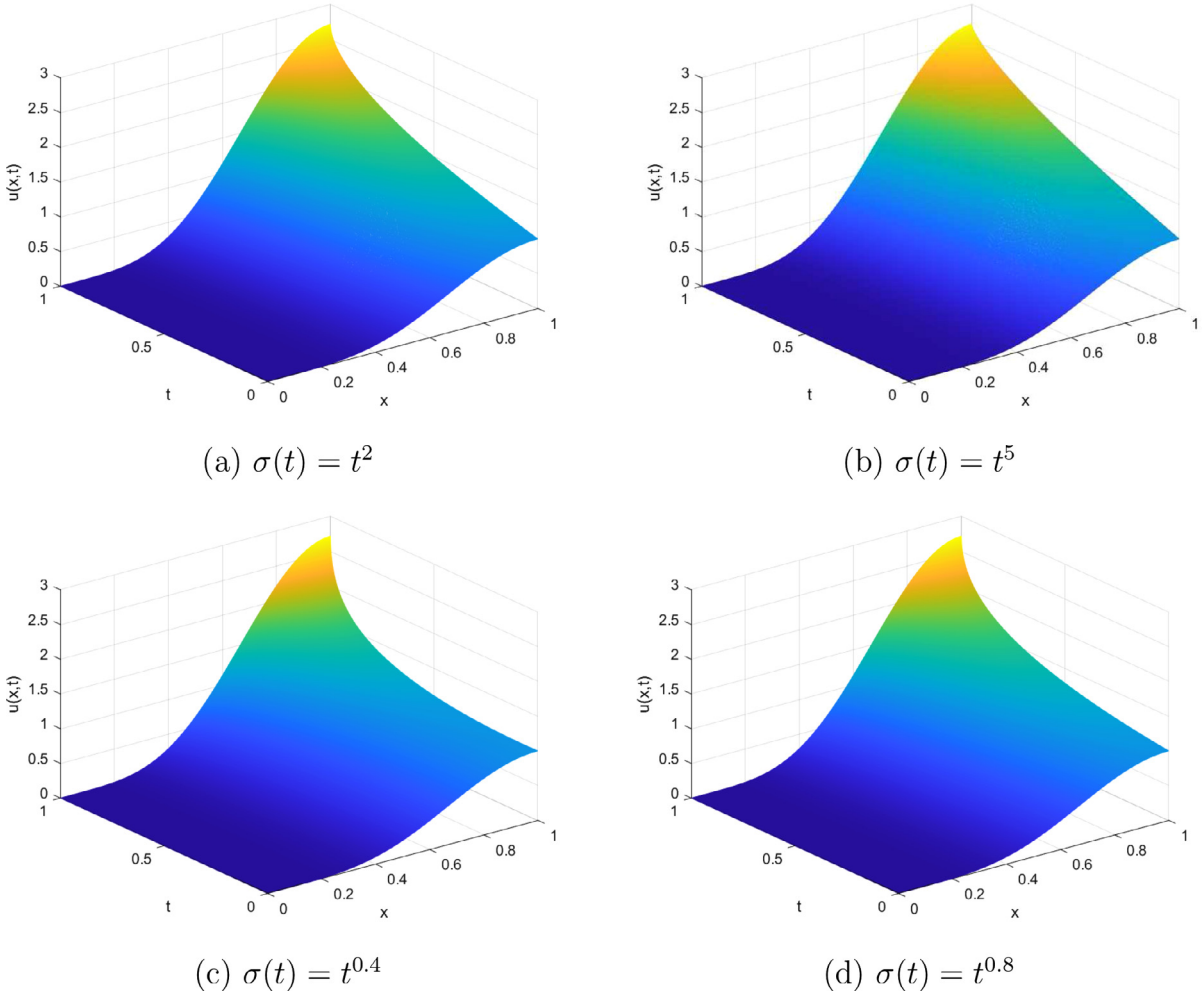

Fig. 6. (Example 4) Numerical solution for fixed step sizes $M = N = 500$, $\alpha = 0.3$, $\omega(t) = 1$ and different values of scale function $\sigma(t)$.

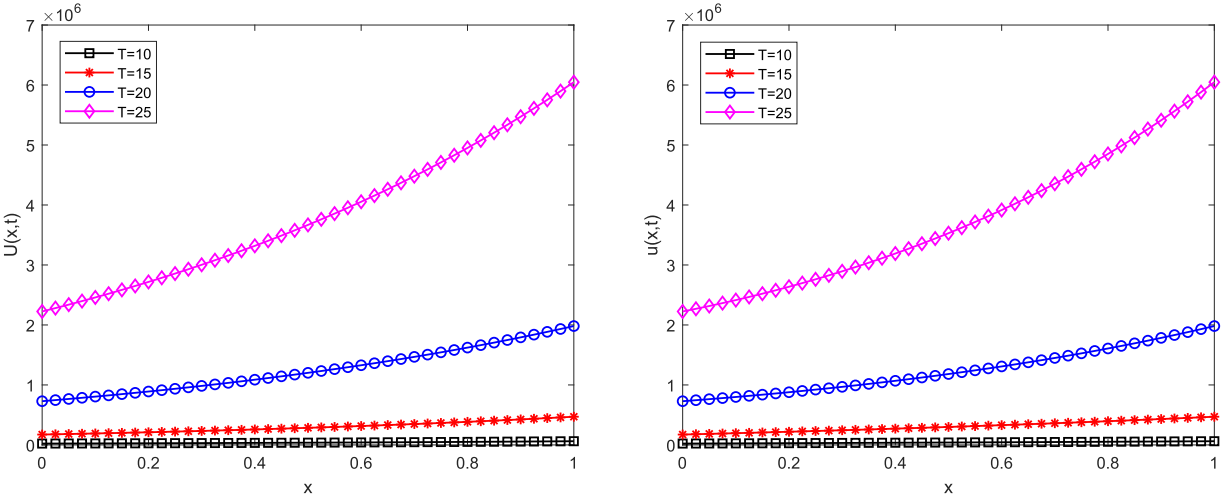

Fig. 7. (Example 4) Exact and numerical solution at different time with $\alpha = 0.5$, $\sigma(t) = t$, $\omega(t) = 1$.

- From Fig. 6(c) and (d), we note that for the stretching scale function $\sigma(t) = t^{0.4}, t^{0.8}$, the solution's behavior is contracting.

Hence, Fig. 6 depicts that the behaviour of the scale function has an inverse effect on the numerical solution of GFTE.

Also, Fig. 7(a) and (b) give the exact and numerical solution plot of the difference scheme at different time $t = T$. The solution curves at $T = 10, 15, 20, 25$ show the efficiency of proposed numerical scheme.

Conclusion

In this paper, we approximated GFD of order $\alpha \in (0, \frac{1}{2}]$ on non-uniform meshes using quadratic interpolation approximation. GFD is described in terms of weight function $\omega(t)$ and scale function $\sigma(t)$. We used a fourth-order compact difference scheme to approximate GFTE on the non-uniform mesh. The temporal and spatial CO of the scheme are observed to be $O(N^{2\alpha-3})$ and 4, respectively. We studied the effect of $\alpha, \omega(t)$, and $\sigma(t)$ on the numerical solution of GFTE. Numerical results verify that the computed order of the numerical accuracy agrees with that of predicted order of accuracy. We showed that our scheme is numerically stable.

Declaration of Competing Interest

The authors declare that they have no known competing financial interests or personal relationships that could have appeared to influence the work reported in this paper.

CRediT authorship contribution statement

Farheen Sultana: Methodology, Software, Writing – original draft. **Rajesh K. Pandey:** Conceptualization, Supervision, Writing – review & editing. **Deeksha Singh:** Writing – original draft, Visualization, Validation. **Om P. Agrawal:** Writing – review & editing.

Acknowledgment

Authors sincerely thank the reviewers for providing constructive comments for improvement of the manuscript.

References

[1] C. Ionescu, A. Lopes, D. Copot, J.T. Machado, J.H. Bates, The role of fractional calculus in modeling biological phenomena: a review, Commun. Nonlinear Sci. Numer. Simul. 51 (2017) 141–159.
[2] R. Hilfer, Applications of Fractional Calculus in Physics, World Scientific, 2000.
[3] A.K. Shukla, R.K. Pandey, S. Yadav, R.B. Pachori, Generalized fractional filter-based algorithm for image denoising, Circuits Syst. Signal Process. 39 (1) (2020) 363–390.
[4] M. Dehghan, Solution of a partial integro-differential equation arising from viscoelasticity, Int. J. Comput. Math. 83 (1) (2006) 123–129.
[5] I. Podlubny, Fractional Differential Equations, Academic Press, San Diego, 1999.
[6] A.A. Kilbas, H.M. Srivastava, J.J. Trujillo, Theory and Applications of Fractional Differential Equations, vol. 204, Elsevier, 2006.
[7] J. Sabatier, O.P. Agrawal, J.T. Machado, Advances in Fractional Calculus, vol. 4, Springer, 2007.
[8] Z. Avazzadeh, M. Heydari, C. Cattani, Legendre wavelets for fractional partial integro-differential viscoelastic equations with weakly singular kernels*, Eur. Phys. J. Plus 134 (7) (2019) 368.
[9] K. Kumar, R.K. Pandey, F. Sultana, Numerical schemes with convergence for generalized fractional integro-differential equations, J. Comput. Appl. Math. 388 (2021) 113318.
[10] C. Li, F. Zeng, Numerical Methods for Fractional Calculus, vol. 24, CRC Press, 2015.
[11] A. Saadatmandi, M. Dehghan, A tau approach for solution of the space fractional diffusion equation, Comput. Math. Appl. 62 (3) (2011) 1135–1142.
[12] J. Ren, Z.-Z. Sun, X. Zhao, Compact difference scheme for the fractional sub-diffusion equation with Neumann boundary conditions, J. Comput. Phys. 232 (1) (2013) 456–467.
[13] O. Abu Arqub, Solutions of time-fractional Tricomi and Keldysh equations of Dirichlet functions types in hilbert space, Numer. Methods Partial Differ. Eqs. 34 (5) (2018) 1759–1780.

[14] A. Alikhanov, M. Beshtokov, M. Mehra, The Crank-Nicolson type compact difference schemes for a loaded time-fractional Hallaire equation, Fract. Calc. Appl. Anal. 24 (4) (2021) 1231–1256.
[15] V.A. Vyawahare, P. Nataraj, Fractional-order modeling of neutron transport in a nuclear reactor, Appl. Math. Model. 37 (23) (2013) 9747–9767.
[16] H. Sun, W. Chen, C. Li, Y. Chen, Fractional differential models for anomalous diffusion, Physica A 389 (14) (2010) 2719–2724.
[17] V. Weston, S. He, Wave splitting of the telegraph equation in R3 and its application to inverse scattering, Inverse Probl. 9 (6) (1993) 789.
[18] P. Jordan, A. Puri, Digital signal propagation in dispersive media, J. Appl. Phys. 85 (3) (1999) 1273–1282.
[19] J. Biazar, M. Eslami, Analytic solution for telegraph equation by differential transform method, Phys. Lett. A 374 (29) (2010) 2904–2906.
[20] S. Momani, Analytic and approximate solutions of the space-and time-fractional telegraph equations, Appl. Math. Comput. 170 (2) (2005) 1126–1134.
[21] M. Ferreira, M.M. Rodrigues, N. Vieira, Fundamental solution of the multi-dimensional time fractional telegraph equation, Fract. Calc. Appl. Anal. 20 (4) (2017) 868–894.
[22] M. Dehghan, A. Shokri, A numerical method for solving the hyperbolic telegraph equation, Numer. Methods Partial Differ.Eqs. Int. J. 24 (4) (2008) 1080–1093.
[23] S. Chen, X. Jiang, F. Liu, I. Turner, High order unconditionally stable difference schemes for the Riesz space-fractional telegraph equation, J. Comput. Appl. Math. 278 (2015) 119–129.
[24] O.P. Agrawal, Some generalized fractional calculus operators and their applications in integral equations, Fract. Calc. Appl. Anal. 15 (4) (2012) 700–711.
[25] Y. Xu, Z. He, O.P. Agrawal, Numerical and analytical solutions of new generalized fractional diffusion equation, Comput. Math. Appl. 66 (10) (2013) 2019–2029.
[26] Y. Xu, O.P. Agrawal, Numerical solutions and analysis of diffusion for new generalized fractional burgers equation, Fract. Calc. Appl. Anal. 16 (3) (2013) 709–736.
[27] Y. Xu, Z. He, Q. Xu, Numerical solutions of fractional advection–diffusion equations with a kind of new generalized fractional derivative, Int. J. Comput. Math. 91 (3) (2014) 588–600.
[28] D. Kong, Y. Xu, Z. Zheng, Numerical method for generalized time fractional KdV-type equation, Numer. Methods Partial Differ. Eqs. 36 (4) (2020) 906–936.
[29] S. Yadav, R.K. Pandey, A.K. Shukla, K. Kumar, High-order approximation for generalized fractional derivative and its application, Int. J. Numer. Methods Heat Fluid Flow 29 (9) (2019) 3515–3534.
[30] K. Kumar, R.K. Pandey, S. Yadav, Finite difference scheme for a fractional telegraph equation with generalized fractional derivative terms, Physica A 535 (2019) 122271.
[31] J. Quintana-Murillo, S. Yuste, A finite difference method with non-uniform timesteps for fractional diffusion and diffusion-wave equations, Eur. Phys. J. Spec. Top. 222 (8) (2013) 1987–1998.
[32] Y.-n. Zhang, Z.-z. Sun, H.-l. Liao, Finite difference methods for the time fractional diffusion equation on non-uniform meshes, J. Comput. Phys. 265 (2014) 195–210.
[33] G.-h. Gao, Z.-z. Sun, H.-w. Zhang, A new fractional numerical differentiation formula to approximate the Caputo fractional derivative and its applications, J. Comput. Phys. 259 (2014) 33–50.
[34] Z. Soori, A. Aminataei, A new approximation to Caputo-type fractional diffusion and advection equations on non-uniform meshes, Appl. Numer. Math. 144 (2019) 21–41.
[35] A. Mohebbi, M. Dehghan, High-order compact solution of the one-dimensional heat and advection–diffusion equations, Appl. Math. Model. 34 (10) (2010) 3071–3084.
[36] L. Li, Z. Jiang, Z. Yin, Fourth-order compact finite difference method for solving two-dimensional convection–diffusion equation, Adv. Differ. Eqs. 2018 (1) (2018) 1–24.
[37] Z. Sun, The Method of Order Reduction and Its Application to the Numerical Solutions of Partial Differential Equations, Science Press, 2009.